A Novel Power Control Strategy for Wind-Driven Permanent Magnet Synchronous Generator Based on a Single Leg Multi-Mode Power Converter

Sertac Bayhan[1,2], *Member, IEEE,* Haitham Abu-Rub[2,3], *Senior Member, IEEE* , and Ilhami Colak[4], *Member, IEEE*
[1]Department of Electronic and Automation, Gazi University, Ankara, Turkey
[2]Department of Electrical and Computer Engineering, Texas A&M University at Qatar, Doha, Qatar
[3]Qatar Environment and Energy Research Institute, Qatar Foundation, Doha, Qatar
[4] Department of Mechatronic Engineering, Istanbul Gelisim University, Istanbul, Turkey
e-mails: sbayhan@gazi.edu.tr, haitham.abu-rub@qatar.tamu.edu, icolak@gelisim.edu.tr

***Abstract*—This paper presents a novel power control strategy for a hybrid power supply system consisting of wind-driven permanent magnet synchronous generator (PMSG) and energy storage device. In this study, a single leg multi-mode power converter, which includes a boost and bidirectional converters to control power flows between energy sources and loads, has been used as a dc/dc converter. This converter has cost effectiveness and fault tolerance features with respect to fewer switches. In order to ensure optimal power flow between energy sources and loads, a novel power control algorithm has been developed. This power control algorithm operates based on input energy from wind turbine, battery state of charge (SOC), and load condition. The proposed system is implemented with Matlab&Simulink software and to verify the performances of the proposed power management control strategy, several simulation studies are performed under different operation conditions. The results show that the proposed system is feasible and applicable.**

***Index Terms*—Power control, single leg multi-mode power converter, permanent magnet synchronous generator (PMSG), energy storage.**

I. Introduction

IN RECENT YEARS, research into the use of renewable energy sources (RES)s has been the subject of increased attention for electricity generation because of increasing environmental awareness and as a consequence of the exhaustible nature of fossil fuels. Among the RESs, wind energy has been regarded as one of the significant energy source. Because, wind energy based power plants have several advantages. Sustainability, pollution free operation and possibility of being installed closer to the end users are just some of these advantages [1], [2]. However, the power obtained from the wind energy often cannot meet the load demand due to the intermittent and stochastic nature of the wind. To cope with this drawback, energy storage systems are essential to maintain energy security, robustness, and stability. To fulfill these targets, an effective energy storage system should be designed to have a high power density as well as a high energy density [3].

In wind energy conversion systems (WECS)s, several electrical machines can be used to implement the electromechanical energy conversion, each of which presents different advantages and disadvantages [4]–[6]. In this study, a permanent magnet synchronous generator (PMSG) is selected as a generator due to its unique advantages: 1) it does not require any reactive power support, 2) it can be driven directly by wind turbine without gearbox, 3) it can be operated in higher power factor and higher efficiency than other generators because of its self-excitation property [7]. However, the performance of the WECSs based on PMSG depends not only on the synchronous generator but also on power electronic interface and how it is controlled. Therefore, to capture maximum power from the wind and to ensure efficient operation of the generator, well-designed power control strategy and power electronic interfaces are required [8].

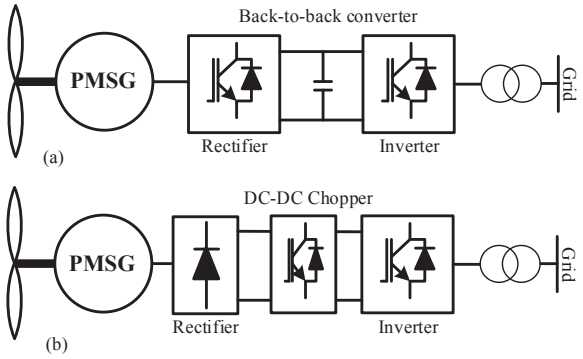

Fig. 1. Traditional PMSG based WECS. (a) Full-scale back-to-back converter system. (b) Diode rectifier with dc-dc converter system.

In general, two types power electronic interface have been used in traditional PMSG based WECS, as shown in Fig. 1. The first topology is called full-scale back-to-back converter that is considered to be a promising PMSG based wind turbine concept, but not yet very popular [9]. However, at the present time, commercial PMSG based wind turbines mainly use a diode rectifier with dc-dc converter configuration because of its simplicity and cost-effective features [10]. In addition to these topologies, recently, new configurations for power electronic interfaces have been reported to provide alternative ways to simplify the system structure and reduce the cost of power conversion components [11]–[17]. One of these topologies is

978-1-4673-6765-3/15/$31.00 ©2015 IEEE

a particular case of the dc-dc converter topology introduced in [17]. In this study, a novel dc-dc converter, which is called single leg multi-mode power converter, was proposed. The major advantage of this topology is that the number of switches is lower than traditional dc-dc converter. As a result of this, converter could be controlled easily and total cost of the power electronic interface was reduced. Because of these advantages, the single leg multi-mode power converter has been selected as a dc-dc converter in this work.

This paper presents a novel power control strategy for wind-driven PMSG based on the single leg multi-mode power converter. The main aim of this study is to improve reliability and stability of the WECSs under variable wind-speed and load variation conditions with a cost-effective power converter topology. The paper is organized as follows: In Section II the mathematical model and operating principle of the single leg multi-mode power converter is explained. The proposed WECS and its controller structure are described in Section III. In Section IV simulation results are presented for different operating conditions. Finally, the conclusion is provided in Section V.

II. Single Leg Multi-mode Power Converter

The single leg multi-mode power converter circuit diagram is given in Fig. 2. This converter can operate in four different modes (main-boost mode, boost-buck mode, boost-boost mode, and battery boost mode) according to input voltage, battery voltage, and desired output voltage . For instance, the input voltage (V_{in}) can be boosted to desired output voltage (V_{out}) value, and battery can be charged or discharged at the same time according to switching signal. Brief analysis of this power converter will be described in this section. A more detailed analysis of this converter, and its characteristics is presented in [17], [18].

A. Main-Boost Mode

The purpose of this mode is to boost an input voltage to a desired output voltage. Two switches (S_1, S_2) are operated with the same switching signals that are illustrated in Fig. 3 (a). In this mode, converter operates like a traditional boost converter and the output voltage of the converter can be written as follows,

$$V_{out} = \frac{1}{1-D} V_{in} \tag{1}$$

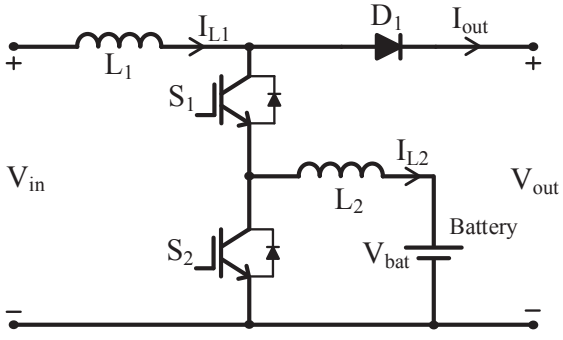

Fig. 2. The single leg multi-mode power converter topology.

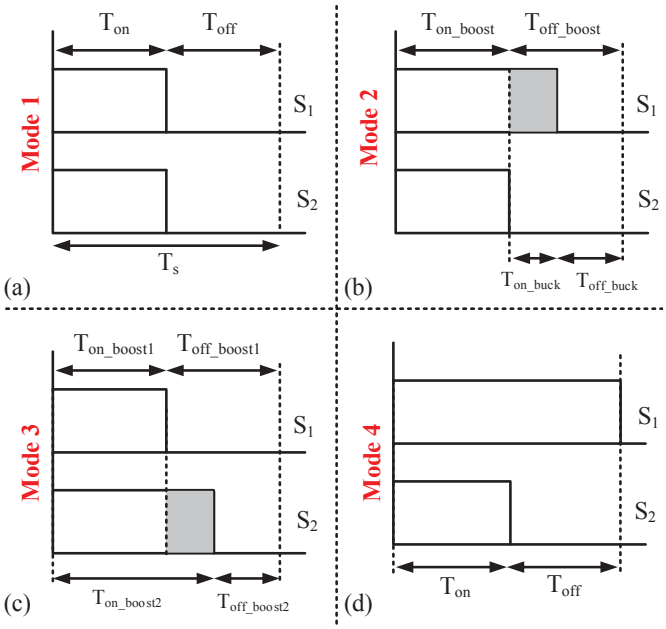

Fig. 3. The switching patterns for all operating modes.

where,

$$D = \frac{T_{on}}{T_s} \tag{2}$$

B. Boost-Buck Mode

In this mode, this converter is able to operate as a boost, and a buck converter at the same switching period. As shown in Fig. 3 (b), the duty cycle of S_1 switching signal is longer than S_2. Thus, the input voltage is boosted to desired output voltage during the T_{on_boost} interval, and the same switching period the battery is charged during the T_{on_buck} interval. To determine the output of the boost converter for this mode, the equations can be given as:

$$V_{out} = \frac{1}{1-D_{boost}} V_{in} \tag{3}$$

where

$$D_{boost} = \frac{T_{on\_boost}}{T_s} \tag{4}$$

to charge the battery, the equations become:

$$V_{bat} = (1-D_{buck}) V_{in} \tag{5}$$

where

$$D_{buck} = \frac{T_{on\_buck}}{T_s} \tag{6}$$

C. Boost-Boost Mode

The purpose of boost-boost mode is to discharge from the battery and to boost the input voltage. It means that converter operates as two boost converters. Fig. 3 (c) depicts that the duty cycle of S_2 switching signal is longer than S_1. Thus, the input voltage is boosted to desired output voltage during the T_{on_boost1} interval, and the same switching period the battery voltage is boosted during the T_{on_boost2} interval. This mode

is used in case of the insufficient input power. The equations for this mode are written as below:

$$V_{out} = \frac{1}{1 - D_{boost1}} V_{in} \tag{7}$$

where

$$D_{boost1} = \frac{T_{on\_boost1}}{T_s} \tag{8}$$

and

$$V_{out} = \frac{1}{1 - D_{boost2}} V_{in} \tag{9}$$

where

$$D_{boost2} = \frac{T_{on\_boost2}}{T_s} \tag{10}$$

D. Battery Boost Mode

Sometimes the input voltage of this converter is very low because of the insufficient input power generation. Therefore, in order to meet power demand, this converter operates as a boost converter in case of this situation, and the battery voltage is boosted to desired output voltage. In this mode, the converter is controlled by S_2 switch to discharge battery. The switching pattern of this mode is illustrated in Fig. 3 (d). The output voltage of this mode can be described in following equations.

$$V_{out} = \frac{1}{1 - D} V_{bat} \tag{11}$$

where

$$D = \frac{T_{on}}{T_s} \tag{12}$$

III. Description of the Proposed System

A. Proposed System Overview

The block diagram of the proposed PMSG based WECS is shown in Fig. 4. The major advantage of PMSG is that it does not require any excitation current from outside. Thus, PMSG can be connected to the dc-dc converter through a three-phase diode rectifier that provides a cost-effective solution. In this scheme, the single leg multi-mode power converter has been used as a dc-dc converter owing to the cost effectiveness and fault tolerance features with respect to fewer switches. Furthermore, to cope with intermittent nature of wind energy and to maintain continuous power to loads, Ni-Cd battery package is connected to the dc link through the same single leg multi-mode power converter. Finally, a three-phase voltage source converter (VSC) is used, so as to provide desired ac voltage for loads.

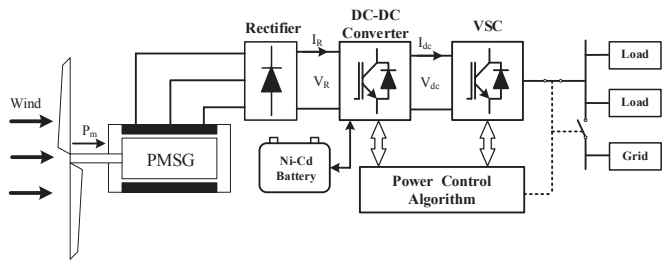

Fig. 4. The proposed wind energy conversion system.

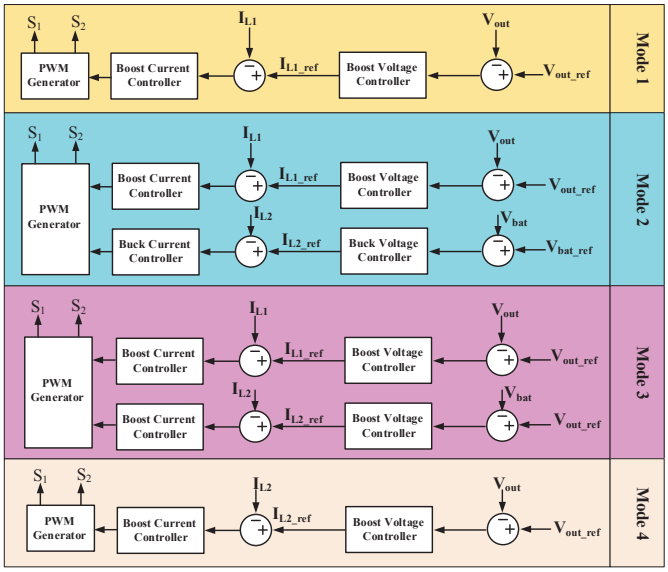

Fig. 5. The control structures of the single leg multi-mode power converter.

B. Proposed Power Control Algorithm

As mentioned in the previous section, the single leg multi-mode power converter can operate in four different modes, depending on the input power source and the battery state of charge (SOC) that is an indication of the energy reserve and it is expressed as follows

$$SOC = 100\left(1 - \frac{\int i_b dt}{Q}\right) \tag{13}$$

where, i_b is the battery current, Q is the battery capacity.

Therefore, this converter requires four different control structures so as to ensure a continuous operation of the proposed WECS. All control structures are given in Fig. 5. In order to select suitable control structure among these, the power control algorithm is developed. The flowchart of this algorithm is shown in Fig. 6. In this algorithm, the energy difference (E_d) value can be expressed as follows

$$E_d = E_w - E_L \tag{14}$$

where, E_w is the energy of wind energy conversion system, and E_L is the energy consumed by the loads. According to

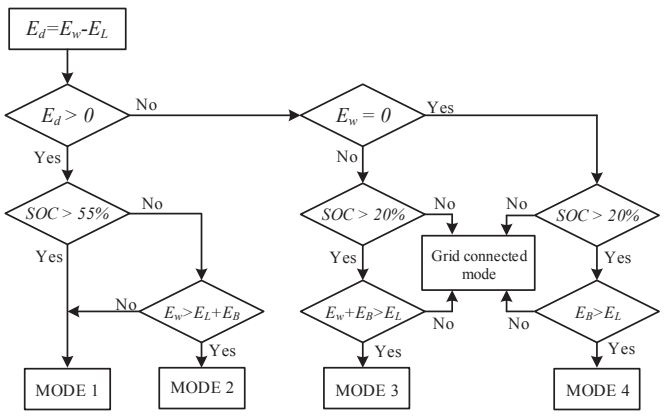

Fig. 6. The flowchart of the power control algorithm.

these parameters, operation of power control algorithm can be described as follows:

- If $E_d > 0$, check the battery SOC. If SOC $>$ 55%, MODE1 (main boost mode) is enabled.
- If the $E_d > 0$ and SOC $<$ 55%, check E_w. If $E_w > E_L + E_B$, MODE2 (boost-buck mode) is enabled. Otherwise, MODE1 is enabled.
- If $E_d < 0$ and $E_w \neq 0$, check the battery SOC. If SOC $>$ 20%, check battery and wind energy. If E_w + $E_B > E_L$, MODE3 (boost-boost mode) is enabled. Otherwise, grid connected mode is enabled.
- If $E_d < 0$ and E_w = 0, check the battery SOC. If SOC $>$ 20%, check battery and load energy. If $E_B > E_L$, MODE4 (battery boost mode) is enabled. Otherwise, grid connected mode is enabled.

In addition to above description, the proposed power control algorithm allows the SOC of the battery to go as low as 20%. Furthermore, with the help of the proposed power control algorithm, all loads can be supplied from the utility grid in case of insufficient input power and/or battery SOC. Thus, the proposed WECS provides continuous power to loads under all conditions.

IV. Simulation Results

The system depicted in Fig. 4 has been implemented in detail using the Matlab&Simulink software. The performance of the system is simulated for different wind and load conditions. The simulation sample time is chosen 25 μs as the converter switching frequency is 10 kHZ. The parameters used in the simulation tests are summarized in Table I in Appendix.

Fig. 7 shows the wind speed and load profile used during the simulation studies. Wind speed changes from 14 to 12 m/s at t=3.25 s, then it changes from 12 to 5 m/s at t=7.25 s. Also, the load demand changes from 6.75 to 5 kW at t=3.25 s, then from 5 to 10 kW at t=5.25 s, lastly from 10 to 5 kW at t=7.25 s. Here, 5 m/s and 16 m/s are the cut-in and rated wind speeds, respectively.

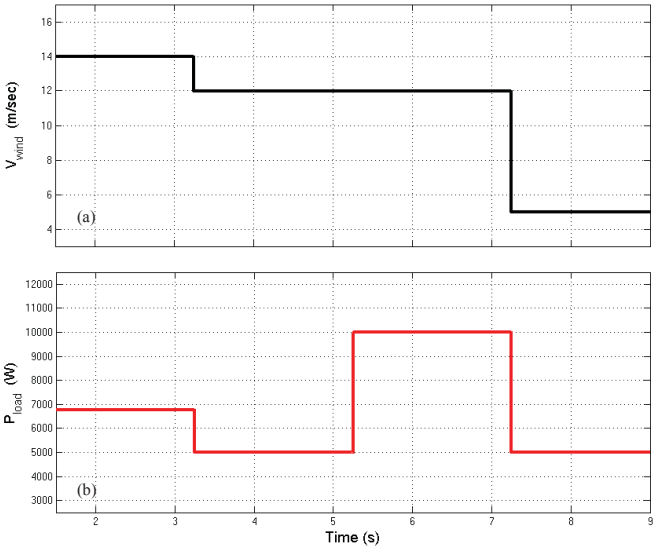

Fig. 7. Wind and load profile during the simulation studies. (a) Wind speed; (b) Load profile.

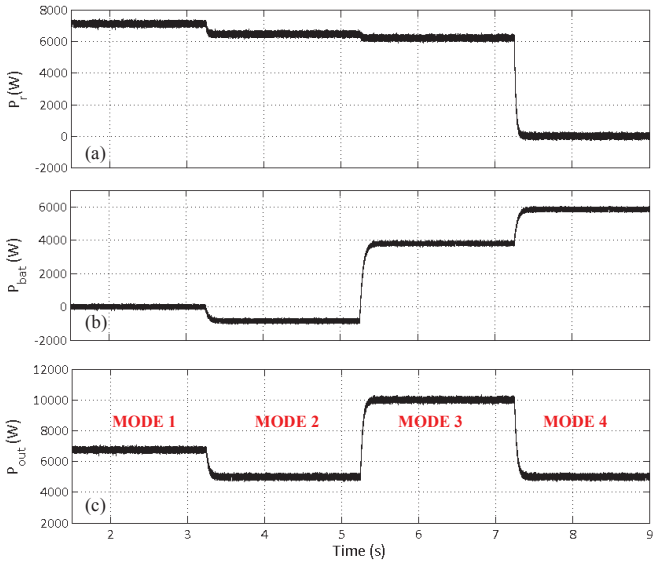

Fig. 8. The proposed system behavior under predefined wind and load profile. (a) rectifier output power; (b) battery power; (c) dc-dc converter output power.

The performance of the proposed WECS under the predefined wind and load profile (see in Fig. 7) is presented in Fig. 8. The rectifier output power ($P_r = V_r.I_r$), battery power ($P_{bat} = V_{bat}.I_{L2}$), and output power of the single leg multi-mode power converter ($P_{out} = V_{dc}.I_{dc}$) are given in Fig. 8(a)-(c), respectively. As can be seen in Fig 8(a), throughout the wind speed variation, the P_r is depends on the wind speed and P_r is 0 W during the $V_{wind} = 5$ m/s that is cut-in speed. However, as can be seen from Fig. 7(b) minimum power demand is 5 kW. Therefore, in order to meet the load demand under various wind speeds and load profile, suitable operating mode must be selected by the proposed power control algorithm to ensure continuous power for the loads. It can be seen from Fig. 8(c), the single leg multi-mode power converter operates in four different modes, with the help of the proposed power control algorithm, to meet load demand.

From Fig. 7(b), till t=3.25 s, the load demand is constant and it is 6.75 kW. During this time, the power obtained from wind turbine is 7.15 kW (see in Fig. 8(a)). As a result, the obtained power from the wind turbine meets load demand and there is no need the battery power. In this condition, the proposed power control algorithm goes to MODE 1 that allows the single leg multi-mode converter to operate in main boost mode (see in Fig. 8(c), between t=1.5 s and 3.25 s).

From Fig. 7(b), at the time 3.25 s, the load decreases from 6.75 to 5 kW. In this condition, the power obtained from wind turbine is more than the load demand ($P_r > P_{out}$). As a result, the excess power ($P_r - P_{out}$) should be stored in the battery. In order to ensure this, the proposed power control algorithm goes to MODE 2 that allows the single leg multi-mode converter to operate in boost-buck mode (see in Fig. 8(c), between t=3.25 s and 5.25 s).

From Fig. 7(b), at the time 5.25 s, the load increases from 5 to 10 kW. In this situation, the obtained power from wind turbine (see in Fig. 8(a)) is less than the load demand. As

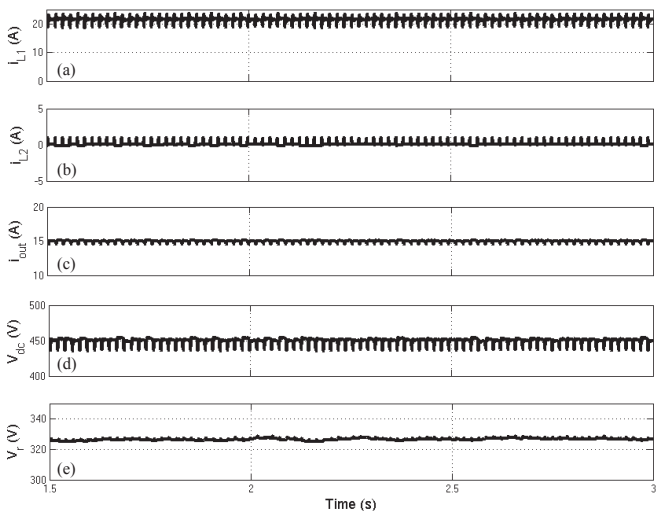

Fig. 9. Simulation results of MODE 1; (a) inductor current (i_{L1}); (b) inductor current (i_{L2}); (c) output current (i_{out}); (d) dc link voltage (V_{dc}); (e) rectifier output voltage (V_r).

a result, in order to ensure the load demand, both battery and wind supply the load. During this situation, the proposed power control algorithm goes to MODE 3 that allows the single leg multi-mode converter to operate in boost-boost mode (see in Fig. 8(c), , between t=5.25 s and 7.25 s).

From Fig. 7(b), at the time 7.25 s, the load decreases from 10 kW to 5 kW. However, at this time wind speed drops 12 to 5 m/s, which is cut-in speed for the wind turbine. In this situation, the obtained power from the wind turbine (see in Fig. 8(a)) is 0 W. Therefore, the load demand must be provided by the battery during this situation to secure the proposed system. As a result, the proposed power control algorithm goes to MODE 4 that allows the single leg multi-mode converter to operate in battery boost mode (see in Fig. 8(c), between t=7.25 s and 9 s).

During this simulation study, the parameters of the single

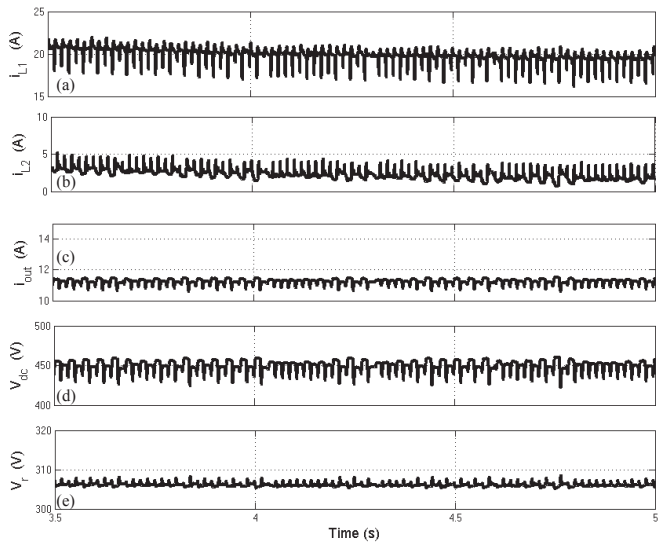

Fig. 10. Simulation results of MODE 2; (a) inductor current (i_{L1}); (b) inductor current (i_{L2}); (c) output current (i_{out}); (d) dc link voltage (V_{dc}); (e) rectifier output voltage (V_r).

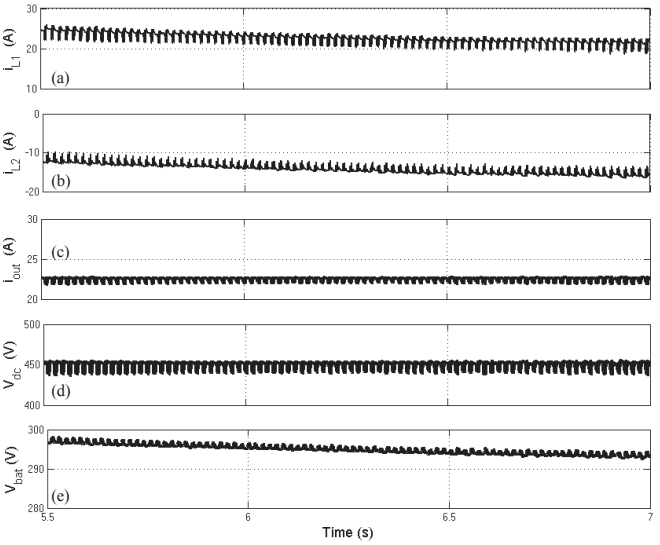

Fig. 11. Simulation results of MODE 3; (a) inductor current (i_{L1}); (b) inductor current (i_{L2}); (c) output current (i_{out}); (d) dc link voltage (V_{dc}); (e) battery voltage (V_{bat}).

leg multi-mode power converter are also examined under four operating modes. Reference of the output dc link voltage is set to 450 V throughout the simulations.

Fig. 9 depicts the simulation results of main boost mode operation (MODE 1), and the inductor currents (i_{L1}) and (i_{L2}), output current (i_{out}), output dc link voltage (V_{dc}), and input dc link voltage (V_r) are given in Fig. 9(a)-(e), respectively. Herein, i_{L2} is 0 A due to there is no need battery power during this operating mode. The load demand is meet entirely by the input source and the V_{dc} is kept constant by the proposed controller (see Fig. 5).

Fig. 10 shows the simulation results of boost-buck mode operation (MODE 2), and the inductor currents (i_{L1}) and (i_{L2}), output current (i_{out}), output dc link voltage (V_{dc}), and

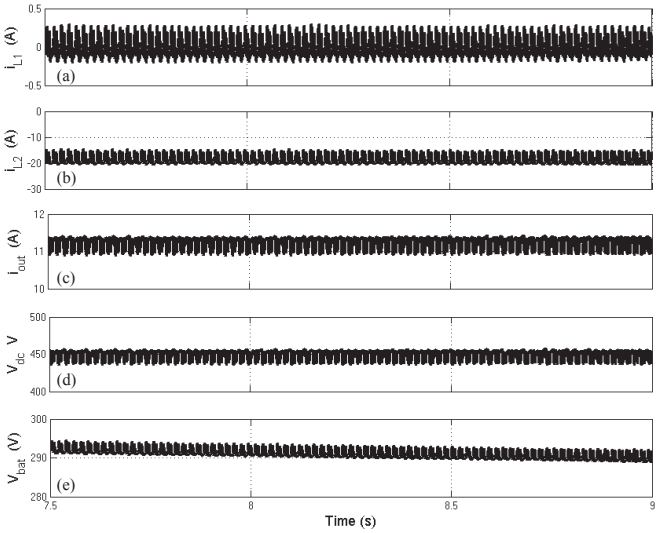

Fig. 12. Simulation results of MODE 4; (a) inductor current (i_{L1}); (b) inductor current (i_{L2}); (c) output current (i_{out}); (d) dc link voltage (V_{dc}); (e) battery voltage (V_{bat}).

Table I
SYSTEM PARAMETERS

PMSG Parameters	
Rated power	7.5 kW
Rated frequency	50 Hz
Winding resistance, R_s	0.42 Ω
Winding inductance, L_s	1.27 mH
Number of Poles	4
DC-DC Converter Parameters	
Inductor (L_1)	1.0 mH
Inductor (L_2)	0.6 mH
Switching frequency	10 KHz
Battery	6 x 48 V, 5Ah
DC link voltage	450 V

input dc link voltage (V_r) are illustrated in Fig. 10(a)-(e), respectively. Here, the battery is charging and charge current i_{L2} is decreasing from 4 A to 2 A. At the same time interval, the V_{dc} is still kept constant by the proposed controller.

Fig. 11 shows the simulation results of boost-boost mode operation (MODE 3), and the inductor currents (i_{L1}) and (i_{L2}), output current (i_{out}), output dc link voltage (V_{dc}), and the battery voltage (V_{bat}) are shown in Fig. 11(a)-(e), respectively. In this mode, in order to meet load demand, the battery has been used as a complementary energy source. As a result, the V_{dc} is still kept constant and the proposed WECS meet load demand under low and insufficient wind energy conditions.

Fig. 12 shows the simulation results of battery boost mode operation (MODE 4), and the inductor currents (i_{L1}) and (i_{L2}), output current (i_{out}), output dc link voltage (V_{dc}), and the battery voltage (V_{bat}) are shown in Fig. 12(a)-(e), respectively. In this mode, i_{L1} is 0 A due to cut-in wind speed. So, there is no input source and, the battery is working as a primary energy source to meet all load demands.

V. CONCLUSION

This paper presents a novel power control strategy for a hybrid power supply system consisting of wind-driven permanent magnet synchronous generator (PMSG) and energy storage device. In this study, a single leg multi-mode power converter, which includes a boost and bidirectional converters to control power flows between energy sources and loads, has been used as a dc/dc converter. The main goal of this study is to ensure load demand under different load and the wind speed conditions. The performance of the proposed WECS is evaluated under different wind and load conditions. The simulation results show that the proposed WECS can provide continuous power to the loads and it can prevent the system from power outages in case of low wind speed and/or insufficient the battery SOC. As a result, the proposed WECS is feasible and applicable.

ACKNOWLEDGMENT

This work was supported by NPRP grant No. 4-077-2-028 from the Qatar National Research Fund (a member of Qatar Foundation). The statements made herein are solely the responsibility of the authors.

APPENDIX

The system parameters used in the simulation studies are indicated in Table I.

REFERENCES

[1] O. Ellabban, H. Abu-Rub, and F. Blaabjerg, "Renewable energy resources: Current status, future prospects and their enabling technology," *Renewable and Sustainable Energy Reviews*, vol. 39, no. 0, pp. 748 – 764, 2014.

[2] H. Abu-Rub, M. Malinowski, and K. Al-Haddad, *Power Electronics for Renewable Energy Systems, Transportation and Industrial Applications*. A John Wiley&Sons Ltd., 2014.

[3] F. Daz-Gonzlez, A. Sumper, O. Gomis-Bellmunt, and R. Villaffila-Robles, "A review of energy storage technologies for wind power applications," *Renewable and Sustainable Energy Reviews*, vol. 16, no. 4, pp. 2154 – 2171, 2012.

[4] H. Polinder, F. van der Pijl, G.-J. de Vilder, and P. Tavner, "Comparison of direct-drive and geared generator concepts for wind turbines," *IEEE Transactions on Energy Conversion*, vol. 21, no. 3, pp. 725–733, Sept 2006.

[5] S. Bayhan, H. Fidanboy, and S. Demirbas, "Active and reactive power control of grid connected permanent magnet synchronous generator in wind power conversion system," in *International Conference on Renewable Energy Research and Applications (ICRERA)*, Oct 2013, pp. 1048–1052.

[6] I. Colak, I. Garip, S. Sagiroglu, and S. Bayhan, "Remote monitoring of the load characteristics of synchronous generators," in *International Conference on Power Engineering, Energy and Electrical Drives (POWERENG)*, May 2011, pp. 1–4.

[7] H. Abu-Rub, A. Iqbal, and J. Guzinski, *High Performance Control of AC Drives with Matlab/Simulink Models*. A John Wiley&Sons Ltd., 2012.

[8] A. Haruni, M. Negnevitsky, M. Haque, and A. Gargoom, "A novel operation and control strategy for a standalone hybrid renewable power system," *IEEE Transactions on Sustainable Energy*, vol. 4, no. 2, pp. 402–413, April 2013.

[9] S. Zhang, K.-J. Tseng, D. Vilathgamuwa, T. D. Nguyen, and X.-Y. Wang, "Design of a robust grid interface system for pmsg-based wind turbine generators," *IEEE Transactions on Industrial Electronics*, vol. 58, no. 1, pp. 316–328, Jan 2011.

[10] K. Amei, Y. Takayasu, T. Ohji, and M. Sakui, "A maximum power control of wind generator system using a permanent magnet synchronous generator and a boost chopper circuit," in *Proceedings of the Power Conversion Conference, PCC-Osaka*, vol. 3, 2002, pp. 1447–1452 vol.3.

[11] K. Nishida, T. Ahmed, and M. Nakaoka, "A cost-effective high-efficiency power conditioner with simple mppt control algorithm for wind-power grid integration," *IEEE Transactions on Industry Applications*, vol. 47, no. 2, pp. 893–900, March 2011.

[12] C. Gu, H. Krishnamoorthy, P. Enjeti, and Y. Li, "A novel medium-frequency-transformer isolated matrix converter for wind power conversion applications," in *IEEE Energy Conversion Congress and Exposition (ECCE)*, Sept 2014, pp. 1070–1077.

[13] Z. Chen, J. Guerrero, and F. Blaabjerg, "A review of the state of the art of power electronics for wind turbines," *IEEE Transactions on Power Electronics*, vol. 24, no. 8, pp. 1859–1875, Aug 2009.

[14] M. Malinowski, S. Stynski, W. Kolomyjski, and M. Kazmierkowski, "Control of three-level pwm converter applied to variable-speed-type turbines," *IEEE Transactions on Industrial Electronics*, vol. 56, no. 1, pp. 69–77, Jan 2009.

[15] Y. Wang, T. Lipo, and D. Pan, "Half-controlled-converter-fed open-winding permanent magnet synchronous generator for wind applications," in *14th International Power Electronics and Motion Control Conference (EPE/PEMC)*, Sept 2010, pp. T4–123–T4–126.

[16] S. Grabic, N. Celanovic, and V. Katic, "Permanent magnet synchronous generator cascade for wind turbine application," *IEEE Transactions on Power Electronics*, vol. 23, no. 3, pp. 1136–1142, May 2008.

[17] T. Park and T. Kim, "Novel energy conversion system based on a multimode single-leg power converter," *IEEE Transactions on Power Electronics*, vol. 28, no. 1, pp. 213–220, Jan 2013.

[18] S. Bayhan, "Labview-based remote laboratory experiments for a multi-mode single-leg converter," *Journal of Power Electronics*, vol. 14, no. 5, pp. 1069–1078, September 2014.